



Comparison of Molecular Structures with DFT and HF of Isoxazoline and Isoxazolidine

Y.S. KARA^{1,*} and S.G. SAGDINC²

¹Department of Chemistry, Science and Art Faculty, Kocaeli University, Umuttepe Campus, 41380 Kocaeli, Turkey

²Department of Physics, Science and Art Faculty, Kocaeli University, Umuttepe Campus, 41380 Kocaeli, Turkey

*Corresponding author: Fax: +90 262 3032003; Tel: +90 262 3032057; E-mail: kara69@gmail.com

(Received: 15 October 2012;

Accepted: 22 July 2013)

AJC-13837

Quantum chemical methods [density functional theory (DFT), *ab initio* (HF) and semi empirical methods] have given to be very important information about the molecular structure in addition to elucidating the electronic structure and reactivity. They have also proved to be a useful tool for studying inhibition mechanisms. In the present study, quantum chemical calculations using the density functional theory and *ab initio* (HF) methods have been performed on three isoxazoline and three isoxazolidine derivatives used as corrosion inhibitors to found the relationship between molecular structure and their inhibition efficiencies. The corresponding structures have been optimized and the highest occupied molecular orbital energy (E_{HOMO}), the lowest unoccupied molecular orbital energy (E_{LUMO}), energy gap (ΔE), electronegativity (χ), hardness (η), softness (σ) and the fraction of electrons transferred from the inhibitor molecule to the metal surface (ΔN) have been calculated using the DFT/B3LYP and HF methods with the 6-31G(d,p) basis set.

Key Words: Corrosion inhibition, DFT, HF, Quantum chemical calculation, Isoxazoline derivatives, Isoxazolidine derivatives.

INTRODUCTION

Heterocycles are an important class of compounds not only due to their natural abundance but also because of their similarities with isoxazoline and isoxazolidine mainly due to their pharmacological activity¹. The isoxazoline derivatives have been reported to possess a variety of significant and diverse pharmacological activities such as antibacterial, anti-candida activity, antifungal, HIV-RT activity²⁻⁶. Similarly, the isoxazolidine derivatives have been published to many pharmacological activities such as antibacterial, antiretroviral drug, hypoglycemic agents, anti-inflammatory, anti-tubercular, anticancer⁷⁻¹². They have been also reported earlier as corrosion inhibitors¹³⁻¹⁴.

Recently Yildirim *et al.*¹⁵ have been investigated experimentally that isoxazoline and isoxazolidine derivatives showed inhibitive properties for iron and its alloys in 2 M HCl solutions 20 h at room temperature. In our previous study, we have performed quantum chemical calculations on acetamides and isoxazolidine derivatives, using the DFT and HF methods¹⁶.

The relationships between the structural parameters and corrosion inhibition of isoxazoline derivatives have not been studied yet. Therefore, the aim of this study is to present theoretical study on electronic and molecular structure of three isoxazoline 5-octylsulfanylmethyl-3-phenyl-4,5-dihydroisoxazol (OSPI), [1-(3-phenyl-4,5-dihydro-isoxazol-5-yl)-nonan-2-ol (PINO), 9-(3-phenyl-4,5-dihydro-isoxazol-5-yl)-nonanoic acid 2-[2-(methoxy-ethoxy)-ethoxy]-ethyl ester

(PINEE)] used as inhibitors and to compare the relationship between some quantum chemical parameters/descriptors from the structures of isoxazoline and isoxazolidine [5-octylsulfanylmethyl-2,3-diphenyl-isoxazolidine (OSDPI), 1-(2,3-diphenyl-isoxazolidin-5-yl)nonan-2-ol (DPINO), 9-(2,3-diphenyl-isoxazolidin-5-yl)nonanoic acid 2-[2-(2-methoxy-ethoxy)-ethoxy]ethyl ester (DPINEE)] and inhibition efficiencies (Table-1).

EXPERIMENTAL

The geometry pre-optimizations of the molecules studied have been carried out by applying the molecular-mechanics method with the MM+ force field using the HyperChem-7.5 software¹⁷. Thereafter, the optimized equilibrium structures of molecules have been calculated at the B3LYP and HF methods 6-31G(d, p) basis set. The corresponding geometries have been optimized without any geometry constraints for full geometry optimizations. The molecules have been built with the GaussView 3.0 visualization program¹⁸ implemented in the Gaussian 03 program package¹⁹.

RESULTS AND DISCUSSION

The calculated quantum chemical parameters such as chemical potential (μ), electronegativity (χ), hardness (η) and softness (σ) were calculated. The concepts of electronegativity (χ)²⁰ and global hardness (η)^{21,22} are given by:

$$\chi = -\mu = -\left(\frac{\partial E}{\partial N}\right)_{v(\vec{r})}$$

$$\eta = \frac{1}{2}\left(\frac{\partial^2 E}{\partial N^2}\right)_{v(\vec{r})} = \frac{1}{2}\left(\frac{\partial \mu}{\partial N}\right)_{v(\vec{r})}$$

where μ is the chemical potential, E is the total energy, N is the number of electrons and $v(\vec{r})$ is the external potential of the system.

The global hardness (η) and chemical potential (μ) were calculated in terms of E_{HOMO} and E_{LUMO} ²³ as:

$$\mu = \frac{E_{\text{HOMO}} + E_{\text{LUMO}}}{2}; \quad \eta = \frac{E_{\text{HOMO}} - E_{\text{LUMO}}}{2}$$

The inverse of the global hardness is designated as the softness, σ as follows:

$$\sigma = 1/\eta$$

The fraction of electrons transferred (ΔN) from the inhibitor molecule to the metallic atom was calculated according to Pearson²⁴⁻²⁶. For a reaction of two systems with different electronegativities (as a metallic surface and an inhibitor molecule) the following mechanism will take place: the electronic flow will occur from the molecule with lower electronegativity toward that of a higher value, until the chemical potentials are the same. In order to calculate the transferred electrons fraction, a theoretical value for the electronegativity of bulk iron was used $\chi_{\text{Fe}}\Psi/\leftarrow 7eV^{24,26}$ and a global hardness of $\eta_{\text{Fe}}: 0$, by assuming that for a metallic bulk I:A²⁷ because they are softer than the neutral metallic atoms. For the calculation the following formula was used^{24,26,28}:

$$\Delta N = \frac{\chi_{\text{Fe}} - \chi_{\text{inh}}}{2(\eta_{\text{Fe}} + \eta_{\text{inh}})}$$

The molecular dipole polarizability α is the linear response of a molecular electronic distribution to the action of an external electric field. In this paper, we are presenting values of mean polarizability (α) as defined in the following equation:

$$\langle \alpha \rangle = \frac{1}{3}(\alpha_{xx} + \alpha_{yy} + \alpha_{zz})$$

and sometimes the anisotropy ($\Delta\alpha$), which is written here in an obvious notation as²⁹.

$$\Delta\alpha = \left\{ \frac{(\alpha_{xx} - \alpha_{yy})^2 + (\alpha_{xx} - \alpha_{zz})^2 + (\alpha_{yy} - \alpha_{zz})^2 + 6(\alpha_{xy}^2 + \alpha_{xz}^2 + \alpha_{yz}^2)}{2} \right\}^{1/2}$$

The α components of the GAUSSIAN 03W output are reported in atomic units, thus the calculated values have to be converted into electrostatic units ($\alpha: 1 \text{ a.u.} = 0.1482 \times 10^{-24} \text{ esu}$)³⁰.

Isoxazoline and isoxazolidine derivatives are bearing three or more of N, O, S heteroatoms and one or two aromatic rings. The compounds are being adsorbed over these heteroatoms and aromatic rings with their π electrons by the metal surface prevent destructive effect of aggressive acidic medium. As known, besides being structures of these heteroatoms, π electrons available in the various functional groups can also facilitate adsorption of corrosion inhibitors to the metal surface and increase inhibition efficiencies¹⁶.

The corrosion efficiencies of inhibitors can be related to their spatial molecular structures and their molecular electronic structures. Adsorption on the metal surface depends on the

structure and the chemical properties of inhibitors. The inhibitor layer has been related to the electronic structure of the molecule. The change and orientation of the inhibitor molecule at the metal surface are also important. Molecular modeling and frontier orbital theory has been proven to help in predicting the adsorption centre of the inhibitors such as the heteroatoms (S, P, N and O), the functions group and electronic density at the donor or acceptor atom π orbital character³¹. In addition to, the planarity and the lonely electron pairs in the heteroatoms are important features that determine the adsorption of these molecules on the metallic surface. Certain quantum chemical parameters that can be related to the metal-inhibitor interaction namely E_{HOMO} , E_{LUMO} , $\Delta E = E_{\text{LUMO}} - E_{\text{HOMO}}$, μ , χ , η , σ , α and ΔN .

The optimized structures, HOMO and LUMO orbitals of isoxazoline and isoxazolidine derivatives are presented in Fig. 1. The spatial distribution of valence electrons is determined by the HOMO orbital, electrophilic attacks can be correlated very well with atomic sites having high density of the HOMO orbital. As can be seen from Fig. 1, the HOMO is found to reside on the benzene ring and heteroatoms for all studied corrosion inhibitors. The figure clearly reveals the information that governs electrophilic attacks on the studied inhibitors.

Table-1 present E_{HOMO} , E_{LUMO} , ΔE , total energy and % inhibition efficiencies for isoxazoline and isoxazolidine derivatives. E_{HOMO} is often associated with the electron donating ability of a molecule. The higher the value of E_{HOMO} of the inhibitor, the greater is the ease of offering electrons to the unoccupied d orbital of metallic iron and the higher is the inhibition efficiency of the inhibitors. E_{LUMO} is lower the value of energy of lowest unoccupied molecular orbital, the easier is the acceptance of electrons from metallic iron surface. Thus higher E_{HOMO} and the lower E_{LUMO} values generally enhance the inhibition efficiency. Moreover, smaller value of ΔE for an inhibitor, higher the inhibition efficiency of that inhibitor³². The calculated E_{HOMO} , E_{LUMO} and $E_{\text{LUMO-HOMO}}$ values for all molecules show that any attempt to correlate parameters with experimental inhibition efficiencies is not significant and there is no simple relation with the inhibition performance of these inhibitors.

Two types of adsorptions are known as physical and chemical adsorption. It can be concluded from the negative sign of the E_{HOMO} obtain in this study that the adsorption these isoxazoline and isoxazolidine derivatives on the steel surface is not by chemical adsorption but by physical adsorption. Physical adsorption results from electrostatic interaction between the charged centres of inhibitor and charged metal surface which results in a dipole interaction of molecules and metal surface³³.

The shape, size, orientation and electronic charge on the molecule determine the degree of adsorption and the effectiveness of the inhibitor. Generally, the inhibition efficiency increases at the molecular weight of the molecules due to the increase of the contact area between corrosion inhibitor molecules and surface. As seen from Table-2, the molecular weights of PINEE and DPINEE are highest of the isoxazoline and isoxazolidine derivatives, respectively, so these molecules are expected the best inhibitors in the isoxazoline and isoxazolidine

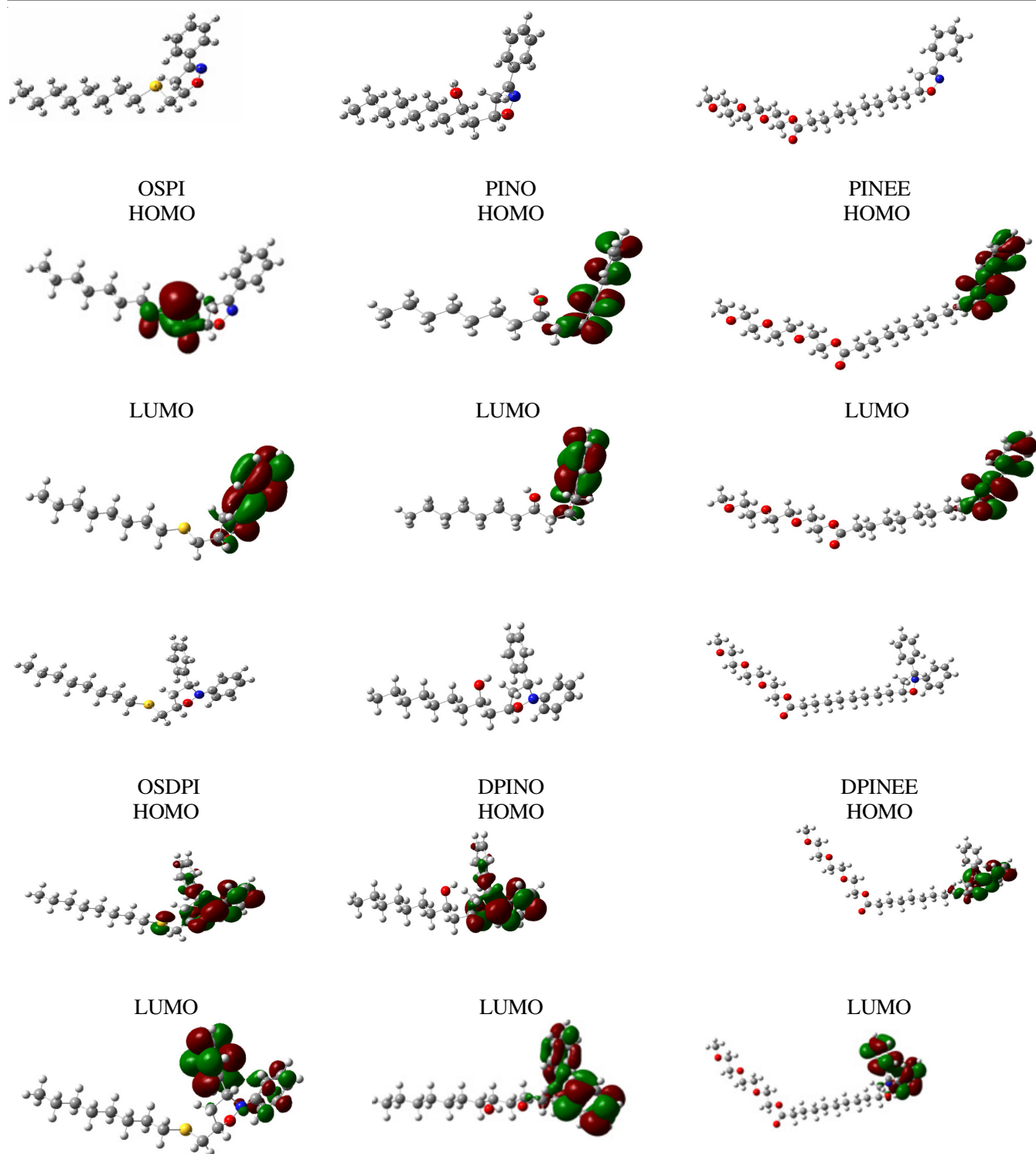


Fig. 1. Molecular structures and HOMO-LUMO of, 5-octylsulfanylmethyl-3-phenyl-4,5-dihydro-isoxazol (OSPI), 1-(3-phenyl-4,5-dihydro-isoxazol-5-yl)-nonan-2-ol (PINO) 9-(3-phenyl-4,5-dihydro-isoxazol-5-yl)-nonanoic acid 2-[2-(methoxy-ethoxy)-ethoxy]-ethyl ester (PINEE), 5-octylsulfanylmethyl-2,3-diphenyl isoxazolidine (OSDPI), 1-(2,3-diphenyl-isoxazolidin-5-yl)-nonan-2-ol (DPINO) 9-(2,3-diphenyl isoxazolidin-5-yl)-nonanoic acid 2-[2-(2-methoxy-ethoxy)-ethoxy]-ethyl ester (DPINEE)

derivatives. However, they have polar ester groups, so they haven't parallel adsorption and their inhibition efficiencies is lower than expected inhibition efficiencies.

PINO and DPINO have same alkyl side chain, but DPINO have second benzene ring in other word a π electron system. A result of this, inhibition efficiency of DPINO is higher than inhibition efficiency of PINO. The HOMO level is mostly

localized on the benzene moiety and O and N atoms in the five membered ring and OH group indicating that preferred sites for electrophilic attack at metal surface are through the O atom (Fig. 1). This means that the benzene moiety with high coefficients of HOMO density was oriented toward the metal surface, so adsorption is probably occurred through the π electrons of benzene moiety, the lone pairs of O and N atoms

TABLE-1
CALCULATED ENERGY (eV) LEVELS OF THE E_{HOMO} , E_{LUMO} , $\Delta E_{\text{HOMO-LUMO}}$, TOTAL ENERGIES AND THE MEASURED AVERAGE INHIBITION EFFICIENCIES (%) AT 50 ppm CONCENTRATION OF 2M HCl SOLUTION¹⁵ FOR THE SERIES OF STUDIED MOLECULES

Molecules		OSPI	PINO	PINEE	OSDPI	DPINO	DPINEE
B3LYP	E_{HOMO}	-5.893	-5.798	-5.892	-5.064	-5.172	-5.264
6-31G(d,p)	E_{LUMO}	-1.041	-0.967	-1.072	-0.094	-0.367	-0.194
	ΔE	4.852	4.831	4.820	4.970	4.806	5.070
	Total Energy	-33479.4	-24691	-40333.5	-39799.3	-31010.9	-46653.4
HF	E_{HOMO}	-8.554	-8.485	-8.577	-7.717	-7.800	-8.034
6-31G(d,p)	E_{LUMO}	2.875	2.939	2.831	3.802	3.643	3.727
	ΔE	11.429	11.424	11.408	11.520	11.443	11.761
	Total Energy	-40154.39	-24531.6	-40083.4	-38526.96	-30809.42	-46361.17
Inhibition eff. (IE) % ^[a] 50 ppm		89.3	56.4	51	91	83.9	88.6

^[a]Ref¹⁵

TABLE-2
MOLECULAR STRUCTURES, ABBREVIATIONS AND MOLECULAR WEIGHTS OF THE ISOXAZOLINE AND ISOXAZOLIDINE DERIVATIVES

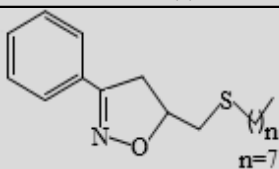
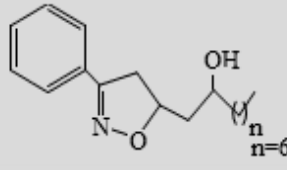
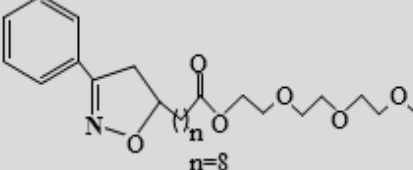
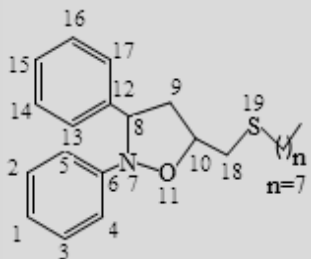
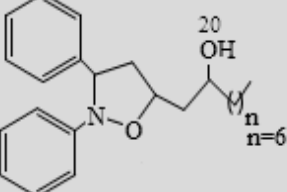
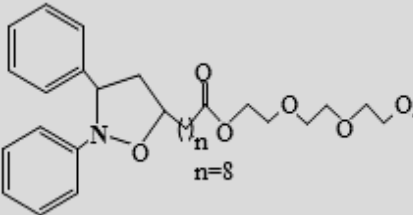
Compounds used as inhibitors	Abbreviation	m.f.	m.w.
1 5-octylsulfanylmethyl-3-phenyl-4,5-dihydro-isoxazol	OSPI		305
2 1-(3-phenyl-4,5-dihydro-isoxazol-5-yl)-nonan-2-ol	PINO		289
3 9-(3-phenyl-4,5-dihydro-isoxazol-5-yl)-nonanoic acid 2-[2-(methoxyethoxy)-ethoxy]-ethyl ester	PINEE		449
4 5-octylsulfanylmethyl-2,3-diphenyl-isoxazolidine	OSDPI		383
5 1-(2,3-diphenyl-isoxazolidin-5-yl)-nonan-2-ol	DPINO		367
6 9-(2,3-diphenyl-isoxazolidin-5-yl)-nonanoic acid 2-[2-(2-methoxyethoxy)-ethoxy]-ethyl ester	DPINEE		527

TABLE-3
HARDNESS (η), SOFTNESS (σ), THE FRACTION OF ELECTRON TRANSFERRED ΔN FOR MOLECULES WITH INHIBITOR PROPERTIES (eV) STUDIED USING DFT AND HF METHODS WITH 6-31G(d,p) BASIS SET IN THE PRESENT WORK

Molecules	η (eV)		σ (1/eV)		ΔN	
	B3LYP 6-31G(d,p)	HF 6-31G(d,p)	B3LYP 6-31G(d,p)	HF 6-31G(d,p)	B3LYP 6-31G(d,p)	HF 6-31G(d,p)
OSPI	2.426	5.715	0.412	0.175	0.728	0.374
PINO	2.416	5.712	0.414	0.175	0.749	0.370
PINEE	2.410	5.704	0.415	0.175	0.730	0.362
OSDPI	2.485	5.760	0.402	0.174	0.889	0.438
DPINO	2.403	5.721	0.416	0.175	0.880	0.430
DPINEE	2.535	5.880	0.394	0.170	0.843	0.412

TABLE-4
MEAN ($\langle\alpha\rangle$) POLARIZABILITIES, THE ANISOTROPY POLARIZABILITIES ($\langle\Delta\alpha\rangle$), THE ELECTRIC DIPOL MOMENTS (μ), THE FIRST-ORDER HYPERPOLARIZABILITIES (β_{tot}) AND THE MEASURED AVERAGE INHIBITION EFFICIENCIES¹⁵ OF THE STUDIED MOLECULES FROM DFT AND HF CALCULATIONS

B3LYP/6-31G(d,p) [HF/6-31G(d,p)]	OSDPI	DPINEE	DPINO	OSPI	PINEE	PINO
$\langle\alpha\rangle \times 10^{-24}$ esu	23.53 (23.68)	34.65 (34.74)	23.83 (24.03)	-19.63 (- 19.73)	-29.79 (-30.10)	-18.62 (-18.80)
$\langle\Delta\alpha\rangle$ au.	14.85 (15.44)	61.31 (59.12)	21.25 (20.59)	3.63 (4.06)	9.8 (9.79)	2.96 (3.52)
Dipole moment (D)	3.80 (3.63)	3.60 (4.14)	1.18 (1.11)	4.24 (4.45)	3.95 (4.99)	2.27 (2.46)
Inhib. eff. % 50 ppm (IE %) ^[15] 50 ppm	89.3	56.4	51	91	83.9	88.6

in the five membered ring and the lone pair of O atom of OH group³⁴.

The optimized structure of isoxazoline derivatives and isoxazolidine derivatives with minimum energies obtain from the calculations are given in Fig. 1. As can be seen from Fig. 1, isoxazolidine derivatives contain second benzene ring different from isoxazoline derivatives. Hence they are more easy dispersion in acidic aqueous medium. As a result of this, the inhibitory properties of the isoxazolidine derivatives more improve than isoxazoline derivatives. The comparison orders of inhibiting efficiency (% IE) are DPINO > PINO, OSDPI > OSPI, DPINEE > PINEE¹⁵.

The sulfur atom on alkyl side chain increases the electron density on the isoxazoline and isoxazolidine derivatives and enhances the inhibition efficiency by strengthening the adsorption interaction. Experimentally, it was found that orders of the inhibition efficiencies (% IE): OSPI > other isoxazoline derivatives and OSDPI > other isoxazolidine derivatives. This was an expected result because of the high electron releasing effect of sulfur atom.

Absolute hardness (η) and softness (σ) are important properties to measure the molecular stability and reactivity. A hard molecule has a large energy gap and a soft molecule has small energy gap. Soft molecules are more reactive than hard ones because they could easily offer electrons to an acceptor. For simplest transfer of electrons, adsorption could occur at the part of the molecule where σ , which is a local property, has the highest³⁵. However, as seen from Table-3, our investigated molecules approximately equal η and σ values. If $\Delta N < 3.6$ (electron), the inhibition efficiency increased electron-donating ability at the metal surface³⁶. DPINO have electron donate group (OH), so ΔN of DPINO higher than other isoxazolidine derivative's ΔN . Calculated values of ΔN are also shown in Table-3.

The dipole moment (μ) is another indicator of the electronic distribution in a molecule and is one of the properties used to discuss and to rationalize the structure³⁷. All the calculated values of dipole moment (μ) and polarizability $\langle\alpha\rangle$ are presented in Table-4. Comparison of the result obtained from quantum chemical calculations with experimental inhibition efficiencies indicated that the % inhibition efficiency of the inhibitors increase with increasing value of the dipole moment. Highest value of μ using B3LYP/6-31G(d,p) method is shown for OSDPI (3.80D) which has the highest inhibition efficiency for isoxazolidine derivatives. Similarly OSPI (4.24D) has the highest inhibition efficiency and highest value of μ in for isoxazoline derivatives. Furthermore, no reasonably good correlation was obtained between polarizability, α and % inhibition efficiency.

Mulliken population analysis³⁸ is mostly used for the calculation of the charge distribution in a molecule. These numerical quantities are easy to obtain and they provide at least a qualitative understanding of the structure and reactivity of molecules. The atomic charges of the studied molecules obtained by Mulliken's population analysis are shown in Table-5. These charges indicate that there is more than one active centre and it is confirmed that the more negative the atomic partial charges of the adsorbed centre is, the more easily the atoms donate its electrons to the unoccupied *d*-orbital of the metal³⁹⁻⁴¹. Recently, good corrosion inhibitors are generally organic compounds which not only offer electrons to unoccupied orbital of the metal but also accept free electrons from the metal⁴². Frontier Orbital Prediction, the site of highest negative density is mainly the site of electrophilic attack. The more negative atomic charges of the adsorbed centers have, the more easily the electrostatic attraction between the surface and studied molecules⁴³. O 20 atom has the most negative charge for DPINO and PINO. Thus the bond with the chelate from

TABLE-5
CHARGES OF C, N, O, S ATOMS FOR STUDIED MOLECULES BY USING B3LYP/6-31G(d,p) AND HF/6-31G(d,p) METHODS

Atoms	B3LYP/6-31G(d,p)			HF/6-31G(d,p)			Atoms	B3LYP/6-31G(d,p)			HF/6-31G(d,p)		
	OSDPI	DPINEE	DPINO	OSDPI	DPINEE	DPINO		OSPI	PINEE	PINO	OSPI	PINEE	PINO
C1	-0.089	-0.085	-0.089	-0.170	-0.161	-0.172	-	-	-	-	-	-	
C2	-0.097	-0.104	-0.094	-0.137	-0.148	-0.137	-	-	-	-	-	-	
C3	-0.095	-0.097	-0.097	-0.138	-0.146	-0.135	-	-	-	-	-	-	
C4	-0.109	-0.093	-0.109	-0.170	-0.138	-0.174	-	-	-	-	-	-	
C5	-0.102	-0.109	-0.112	-0.163	-0.173	-0.174	-	-	-	-	-	-	
C6	0.292	0.280	0.287	0.293	0.284	0.291	-	-	-	-	-	-	
N7	-0.308	-0.320	-0.301	-0.381	-0.390	-0.376	N7	-0.189	-0.190	-0.202	-0.147	-0.147	-0.166
C8	0.020	-0.419	-0.429	0.094	0.105	0.097	C8	0.244	0.232	0.244	0.262	0.248	0.273
C9	-0.244	-0.238	-0.251	0.289	0.135	-0.294	C9	-0.284	-0.283	-0.283	-0.315	-0.306	-0.302
C10	0.237	0.200	0.219	0.269	0.252	0.254	C10	0.170	0.187	0.156	0.218	0.247	0.203
O11	-0.409	-0.419	-0.429	-0.524	-0.540	-0.543	O11	-0.394	-0.410	-0.405	-0.523	-0.543	-0.535
C12	0.123	0.093	0.132	-0.020	-0.042	-0.014	C12	0.109	0.111	0.105	-0.038	-0.036	-0.044
C13	-0.130	-0.121	-0.122	-0.163	-0.157	-0.157	C13	-0.107	-0.108	-0.110	-0.122	-0.123	-0.125
C14	-0.086	-0.088	-0.083	-0.136	-0.145	-0.140	C14	-0.091	-0.091	-0.092	-0.155	-0.154	-0.155
C15	-0.085	-0.084	-0.083	-0.149	-0.153	-0.153	C15	-0.088	-0.081	-0.082	-0.143	-0.143	-0.144
C16	-0.085	-0.087	-0.082	-0.146	-0.145	-0.144	C16	-0.091	-0.091	-0.092	-0.153	-0.153	-0.154
C17	-0.088	-0.108	-0.169	-0.151	-0.137	-0.188	C17	-0.136	-0.138	-0.136	-0.157	-0.159	-0.154
C18	-0.377	-0.182	-0.206	-0.412	-0.219	-0.237	C18	-0.331	-0.187	-0.179	-0.383	-0.227	-0.217
S19	0.099	-	-	0.135	-	-	S19	0.102	-	-	0.146	-	-
O20	-	-	-0.554	-	-	-0.666	O20	-	-	-0.553	-	-	-0.666

O20 [-0.554 for B3LYP/6-31G(d,p), -0.666 for HF/6-31G(d,p) DPINO and -0.553 for B3LYP/6-31G(d,p), -0.666 for HF/6-31G(d,p) PINO] will be easily formed, rather than other atoms. The calculation shows that N7, C9, O11 and C18 are high negative charges for isoxazoline and isoxazolidine derivatives. Hence these atoms are the most probable centres of adsorption *via* the lone pair electrons in studied molecules. The sulphur atom present positive charges, being the further value of 0.102 for B3LYP/6-31G(d,p), 0.146 for HF/6-31G(d,p) for the sulphur atom of OSPI, thus probably experiencing the greater repulsive effect towards metallic atom when the molecule acts as a nucleophile and the less value of the positive charge being 0.099 for B3LYP/6-31G(d,p), 0.135 for HF/6-31G(d,p) for the sulphur atom of OSDPI. This makes the OSDPI to probably experience the greatest attractive effect towards metallic atoms when molecule acts as a nucleophile thus making it to probably exhibit the highest inhibitive effect. Similar observation has been reported by Obot *et al.*⁴⁴ on their study of hard & soft acid base descriptors of thiazazole derivatives calculated by DFT: possible relationship as mild steel corrosion inhibitors.

Conclusion

The comparison between the quantum chemical parameters of isoxazoline and isoxazolidine derivatives was calculated using the density functional theory (DFT) and *ab initio* (HF) methods. The quantum chemical parameters of six different molecules indicate that the inhibition effect of isoxazoline and isoxazolidine derivatives is no simple relation with the inhibition performance of these inhibitors. The inhibition efficiency increased with the increase in dipole moment and ΔN . Isoxazolidine derivatives have second benzene ring in other word a π electron system. A result of this, inhibition efficiency of isoxazolidine is higher than inhibition efficiency of isoxazoline.

Mulliken population analysis shows, that the mechanism of adsorption between the isoxazoline and isoxazolidine derivatives and mild steel surface occurs mainly through the same atoms (N7, C9, O11, C18) not the sulphur atom.

REFERENCES

- S.B. Jadhav, R.A. Shastri, K.V. Gaikwad and S.V. Gaikwad, *E.-J. Chem.*, **6(S1)**, 183 (2009).
- T. Shah and V. Desai, *J. Serb. Chem. Soc.*, **72**, 443 (2007).
- M.B. Gravestock, N.J. Hales, M.L. Swain, S.I. Hauck and S.D. Mills. Oxazolidinone and/or Isoxazoline as Antibacterial Agents, US Patent, 7,396,847 (2008).
- P.C. Sharma, S.V. Sharma, S. Jain, D. Singh and B. Suresh, *Acta Pol. Pharm.*, **66**, 101 (2009).
- M. Imran and S.A. Khan, *Indian J. Heterocycl. Chem.*, **13**, 213 (2004).
- P. Zhang, C. Wei, E. Wang, W. Wang, M. Liu, Q. Yin, H. Chen, K. Wang, X. Li and J. Zhang, *Carbohydr. Res.*, **351**, 7 (2012).
- P.V. Tekade, K.N. Patil and P.S. Bodkhe, *Asian J. Chem.*, **17**, 1340 (2005).
- B. Loh, L. Vozzolo, B.J. Mok, C.C. Lee, R.J. Fitzmaurice, S. Caddick and A. Fassati, *Chem. Biol. Drug Des.*, **75**, 461 (2010).
- H. Shinkai, S. Onogi, M. Tanka, T. Shibata, M. Iwao, K. Wakitani and I. Uchida, *J. Med. Chem.*, **41**, 1927 (1998).
- M.P. Sadashiva, A. Nataraju, H. MalleshA, B.S. Vishwanath and K.S. Rangappa, *Int. J. Mol. Med.*, **16**, 895 (2005).
- R.V. Kumar, S. Mukherjee, P. A.K. Prasad, C.E. Olsen, S.J.C. Schaffer, S.K. Sharma, A.C. Watterson, W. Errington and V.S. Parmar, *Tetrahedron*, **61**, 5687 (2005).
- R. Singh, S.D. Bhella, A.K. Sexana, M. Shanmugavel, A. Faruk and M.P.S. Ishar, *Tetrahedron*, **63**, 2283 (2007).
- S.A. Ali, A.M. El-Shareef, R.F. Al-Ghamdi and M.T. Saeed, *Corros. Sci.*, **47**, 2659 (2005).
- S.A. Ali, M.T. Saeed and S.U. Rahman, *Corros. Sci.*, **45**, 253 (2003).
- A. Yildirim and M. Çetin, *Corros. Sci.*, **50**, 155 (2008).
- Y.S. Kara, S.G. Sagdinc and A. Esme, *Prot. Met. Phys. Chem. Surf.*, **48**, 710 (2012).
- HyperChem 7.5 Release for Windows, Hypercube Inc., USA, (2003).
- A. Frisch, A.B. Nielsen and A.J. Holder, GaussView Users Manual, Gaussian Inc., Pittsburg (2000).
- M.J. Frisch, G.W. Trucks, H.B. Schlegel, G.E. Scuseria, M.A. Robb, J.R. Cheeseman, J.A. Montgomery, T. Vreven, K.N. Kudin, J.C. Burant, J.M. Millam, S.S. Iyengar, J. Tomasi, V. Barone, B. Mennucci, M. Cossi,

- G. Scalmani, N. Rega, G.A. Petersson, H. Nakatsuji, M.M. Ehara, K. Toyota, R. Fukuda, J. Hasegawa, M. Ishida, T. Nakajima, Y. Honda, O. Kitao, H. Nakai, M. Klene, X. Li, J.E. Knox, H.P. Hratchian, J.B. Cross, V. Bakken, C. Adamo, J. Jaramillo, R. Gomperts, R.E. Stratmann, O. Yazyev, A.J. Austin, R. Cammi, C. Pomelli, J.W. Ochterski, P.Y. Ayala, K. Morokuma, G.A. Voth, P. Salvador, J.J. Dannenberg, V.G. Zakrzewski, S. Dapprich, A.D. Daniels, M.C. Strain, O. Farkas, D.K. Malick, A.D. Rabuck, K. Raghavachari, J.B. Foresman, J.V. Ortiz, Q. Cui, A.G. Baboul, S. Clifford, J. Cioslowski, B.B. Stefanov, G. Liu, A. Liashenko, P. Piskorz, I. Komaromi, R.L. Martin, D.J. Fox, T. Keith, M.A. Al-Laham, C.Y. Peng, A. Nanayakkara, M. Challacombe, P.M. W. Gill, B. Johnson, W. Chen, M.W. Wong, C. Gonzalez, J.A. Pople, Gaussian 03, Revision B.05, Gaussian, Inc., Wallingford, CT (2004).
20. R.G. Parr, D.A. Donnelly, M. Levy and M. Palke, *J. Chem. Phys.*, **68**, 3801 (1978).
21. R.G. Parr and R.G. Pearson, *J. Am. Chem. Soc.*, **105**, 7512 (1983).
22. R.G. Pearson, *Inorg. Chem.*, **27**, 734 (1998).
23. B. Gomez, N.V. Likhanova, M.A. Dominguez-Aguilar, R. Martinez-Palou, A. Vela and J.L. Gazquez, *J. Chem. Phys.*, **B110**, 8928 (2006).
24. V.S. Sasti and J.R. Perumareddi, *Corrosion*, **53**, 617 (1997).
25. I. Lukovits, E. Kalman and F. Zucchi, *Corrosion*, **57**, 3 (2001).
26. S. Martinez, *Mater. Chem. Phys.*, **77**, 97 (2002).
27. M.J.S. Dewar and W. Thiel, *J. Am. Chem. Soc.*, **99**, 4899 (1977).
28. L.M. Rodriguez-Valdez, W. Villamizar, M. Casales, J.G. Gonzalez-Rodriguez, A. Martinez-Villafane, L. Martinez and D. Glossman-Mitnik, *Corros. Sci.*, **48**, 4053 (2006).
29. G.J. Avila, *J. Chem. Phys.*, **122**, 144310 (2005).
30. A.B. Ahmed, H. Feki, Y. Abid, H. Boughzala and A. Mlayah, *J. Mol. Struct.*, **888**, 180 (2008).
31. N.O. Eddy and E.E. Ebenso, *Int. J. Electrochem. Sci.*, **5**, 731 (2010).
32. I. Ahamad, R. Prasad and M.A. Quraishi, *Corros. Sci.*, **52**, 933 (2010).
33. T. Arslan, F. Kandemirli, E.E. Ebenso, I. Love and H. Alemu, *Corros. Sci.*, **51**, 35 (2009).
34. M.S. Masoud, M.K. Awad, M.A. Shaker and M.M.T. El-Tahawy, *Corros. Sci.*, **52**, 2387 (2010).
35. S. Martinez, *Mater. Chem. Phys.*, **77**, 97 (2002).
36. H. Ju, Z.-P. Kai and Y. Li, *Corros. Sci.*, **50**, 865 (2008).
37. O. Kikuchi, *Quant. Struct.-Act. Relat.*, **6**, 179 (1987).
38. R.S. Mulliken, *J. Chem. Phys.*, **23**, 1833 (1955).
39. K.F. Khaled, *Electrochim. Acta*, **53**, 3484 (2008).
40. K.F. Khaled and M.A. Amin, *J. Appl. Electrochem.*, **38**, 1609 (2008).
41. J.M. Roque, T. Pandiyan, J. Cruz and E. Gracia-Ochoa, *Corros. Sci.*, **50**, 614 (2008).
42. E.E. Ebenso, T. Arslan, F. Kandemirli, I. Love, C. Ögretir, M. Saracoglu and S.A. Umoren, *Int. J. Quantum. Chem.*, **110**, 2614 (2010).
43. G. Gece, S. Bilgiç and Ö. Türksen, *Mater. Corros.*, **61**, 141 (2010).
44. I.B. Obot and N.O. Obi-Egbedi, *Der Pharma Chem.*, **1**, 151 (2009).